

Geophysical Research Letters

RESEARCH LETTER

10.1029/2021GL094696

Key Points:

- We identified a conjunction between the low Earth orbiting Solar Anomalous and Magnetospheric Particle Explorer (SAMPEX) satellite and a Time History of Events and Macroscale Interactions during Substorms (THEMIS) all-sky imager at Gillam, Canada
- We found a high correlation between patchy aurora and >1 MeV electron microburst precipitation observed during the conjunction
- This correlation suggests a close connection between relativistic electron microbursts and patchy aurora

Supporting Information:

Supporting Information may be found in the online version of this article.

Correspondence to:

M. Shumko,
msshumko@gmail.com

Citation:

Shumko, M., Gallardo-Lacourt, B., Halford, A. J., Liang, J., Blum, L. W., Donovan, E., et al. (2021). A strong correlation between relativistic electron microbursts and patchy aurora. *Geophysical Research Letters*, 48, e2021GL094696. <https://doi.org/10.1029/2021GL094696>

Received 8 JUN 2021

Accepted 24 AUG 2021

A Strong Correlation Between Relativistic Electron Microbursts and Patchy Aurora

M. Shumko^{1,2} , B. Gallardo-Lacourt^{1,2} , A. J. Halford¹ , J. Liang³ , L. W. Blum⁴ , E. Donovan³, K. R. Murphy , and E. L. Spanswick³ 

¹NASA's Goddard Space Flight Center, Greenbelt, MD, USA, ²Universities Space Research Association, Columbia, MD, USA, ³University of Calgary, Calgary, AB, Canada, ⁴University of Colorado Boulder, Boulder, CO, USA

Abstract In this letter, we present the results of a conjunction between the Solar Anomalous and Magnetospheric Particle Explorer (SAMPEX) satellite and a Time History of Events and Macroscale Interactions during Substorms (THEMIS) all-sky imager in Gillam, Canada, showing a high correlation between relativistic, >1 MeV, electron microbursts and a type of pulsating aurora called patchy aurora. The correlation was 0.8, and is not serendipitous. While the relationship between pulsating aurora and 10–100s keV microbursts has been previously predicted, here we show a strong association between keV and MeV electron dynamics, possibly spanning two orders of magnitude. Importantly, this result shows that the dynamics of relativistic radiation belt electrons are at times intimately tied to keV electron precipitation, and cannot be studied in isolation.

Plain Language Summary In this letter, we present a coordinated observation between a low Earth orbiting satellite, orbiting at 400 km altitude above Earth's surface, and an auroral all-sky imager in Canada. This observation showed a connection of a type of pulsating aurora, called patchy aurora, with extremely energetic and intense bursts of electron radiation called microbursts. This link is surprising because the electron energies responsible for auroral light are 100 times lower than the electrons that were directly observed in space. Our result implies that the mechanism responsible for patchy aurora and microbursts is likely the same, and could be capable of affecting electrons with vastly different energies. This result is a major step toward unifying the microburst and patchy aurora phenomena and shows that the dynamics of high-energy electrons located in near-Earth space can be intimately tied to much lower energy electron precipitation, and must therefore be studied together.

1. Introduction

Energetic electrons in Earth's magnetosphere are highly dynamic, governed by a complex interplay of many source and loss mechanisms (e.g., Ripoll et al., 2020, and references therein). One important loss mechanism is the interaction between electrons and plasma waves, resulting in precipitation of electrons into Earth's upper atmosphere (e.g., Breneman et al., 2017; Lorentzen, Looper, & Blake, 2001; Thorne et al., 2005).

These precipitating electrons can cause various types of auroral displays including pulsating aurora, a form of diffuse aurora characterized by a diverse variation of irregular shapes, sizes, and pulsating frequencies (Grono & Donovan, 2020; Johnstone, 1978; Lessard, 2012; Royrvik & Davis, 1977). An individual pulsating aurora patch is typically 10–200 km across, while the entire pulsating aurora region can extend over at least 10 h of magnetic local time (Johnstone, 1978; Jones et al., 2013). In the literature, pulsating aurora frequencies are often studied in two categories: the on-off pulsations that last 2–20 s (e.g., Johnstone, 1978) and the faster, ≈ 3 Hz modulations that are superposed on the on-off pulsations (Hoffman & Evans, 1968; Nishiyama et al., 2012; Royrvik & Davis, 1977). Moreover, even higher frequency modulations of 54 Hz have been observed by a high-speed camera (Kataoka et al., 2012).

Quantifying the energy of the precipitating electrons is important for understanding the drivers and dynamics of pulsating aurora. Observations of pulsating aurora, together with atmospheric models or satellite observations, are some of the ways used to estimate the precipitating electron energies. Brown et al. (1976) used triangulation to estimate the emission altitude of pulsating aurora. The authors found the mean lower-bound altitude of pulsating aurora of 92 km, with a range of 82–105 km, concluding that the electrons capable of penetrating that deep into the atmosphere have 10–60 keV energies. Samara et al. (2015) presented

measurements from low Earth orbiting satellites, made in conjunction with All-Sky Imagers (ASIs), and found that pulsating aurora electrons typically have 3–20 keV energies, and at times up to 30 keV. Nonetheless, pulsating aurora can have even higher electron energies. A Substorm-GEOS rocket that launched into pulsating aurora in 1979 directly observed pulsating aurora electrons in the >140 keV integral energy channel (Sandahl et al., 1980). More recently, Miyoshi et al. (2015) estimated the upper energy bound of pulsating aurora using an ASI and a very high frequency radar at Tromsø, Norway; pulsating aurora was observed by the ASI, while the radar observed a substantial electron density enhancement at altitudes as low as 68 km, corresponding to 200 keV electrons (e.g., Fang et al., 2010). These authors concluded that the keV pulsating aurora can be associated with subrelativistic and relativistic electron precipitation. Together, these observations suggest that the electrons that produce pulsating aurora likely represent only a portion of the precipitating electron spectra (Tesema et al., 2020). Thus, the upper energy bound is still unknown.

Several driving mechanisms of the electron precipitation responsible for pulsating auroras have been evaluated. The drivers are still under intense debate, but the two primary candidates are: electrostatic cyclotron harmonic (ECH) and whistler-mode chorus waves (Fukizawa et al., 2018; Horne et al., 2005; Summers, 2005). Whistler-mode chorus, subsequently referred to as chorus, are commonly characterized by their rising or falling tone elements (Omura & Nunn, 2011; Tsurutani & Lakhina, 1997). Chorus waves are typically right-hand circularly polarized, with frequencies in between 0.1 – 1 of the electron gyrofrequency, f_{ce} . In frequency, chorus waves are further split up into upper and lower bands with a break at $0.5f_{ce}$ (Li et al., 2019). Upper-band chorus is typically effective at scattering <3 keV electrons, while lower-band chorus is effective at scattering >10 keV electrons (Thorne et al., 2010).

Recent modeling and conjunction observations favor chorus waves scattering electrons (Miyoshi et al., 2015; Nishimura et al., 2010; Thorne et al., 2010) near the magnetic equator (Jaynes et al., 2013; Kasahara et al., 2018). Nonetheless, the relation between chorus and pulsating aurora remains an important topic of study, notably due to the relation between chorus waves and radiation belt dynamics and the range of electron energies spanning these observations, from several keV to multiple MeV. Furthermore, at these high energies, precipitating electrons can strongly affect atmospheric chemistry (Duderstadt et al., 2021).

Prior studies have also reported another form of electron precipitation in this energy range (10s KeV–MeV) called electron microbursts. Microbursts are typically defined as a subsecond intense increase of energetic electron precipitation into Earth's atmosphere and are also believed to be scattered by chorus waves (Breneman et al., 2017; Crew et al., 2016; Lorentzen, Blake, et al., 2001; O'Brien et al., 2004; Tsurutani et al., 2013). Microbursts were first coined by Anderson and Milton (1964), who used high-altitude balloon data to characterize the subsecond enhancements of >25 keV X-rays, emitted by precipitating electrons. Microbursts were observed in isolation as well as in groups of three or more microbursts in rapid succession called microburst trains. Since then, keV–MeV microbursts were directly and indirectly observed by balloons, sounding rockets and satellites (e.g., Blum et al., 2015; Datta et al., 1997; Douma et al., 2017; Millan & Thorne, 2007; Woodger et al., 2015).

Similar to pulsating aurora, the observational link between chorus and microbursts is widely accepted. Oliven and Gurnett (1968) found that >40 keV microbursts were always accompanied by chorus waves. However, a one-to-one correspondence was not found. More recently, Breneman et al. (2017) studied a conjunction where chorus rising tone elements likely scattered 100s keV microbursts because they had a similar repetition rate and duration. Together with statistical studies (e.g., Lorentzen, Blake, et al., 2001; O'Brien et al., 2003), this body of work has established a compelling relation between chorus waves and microburst electron precipitation.

With the aforementioned chorus-pulsating aurora and chorus-microburst relationships, pulsating aurora and microbursts, especially relativistic microbursts, are often studied independently, and only occasionally their relationship is considered. An exception is Hofmann and Greene (1972). The authors used data from a balloon that carried a photometer and a scintillator that showed correlation between violet light and >20 keV X-ray modulation on both the on-off and modulation time scales. The upper energy of the precipitation was 50 keV as the >50 keV scintillator channel did not respond. Hofmann and Greene (1972) classified the subsecond >20 keV X-ray modulations as microbursts.

The link between pulsating aurora and relativistic microbursts is observationally elusive, but has been theoretically proposed. Recent test-particle simulations by Chen et al. (2020) and Miyoshi et al. (2020) show that whistler-mode chorus rising tone elements can scatter keV–MeV microburst electrons. Miyoshi et al. (2020) went on to hypothesize that relativistic microbursts are the high-energy tail of pulsating aurora. However, the observational association of MeV electron microbursts with pulsating aurora is unreported. This is likely due to several factors including difficulties finding good conjunctions between satellites and ground-based imagers capable of observing both phenomena, and the small size of individual pulsating aurora patches and microbursts (Blake et al., 1996; Grono & Donovan, 2020; Johnstone, 1978; Shumko et al., 2020).

In this letter, we present observational evidence supporting a link between pulsating aurora and relativistic (>1 MeV) microburst electron precipitation. We showcase a conjunction between a Time History of Events and Macroscale Interactions during Substorms (THEMIS) ASI at Gillam, Canada and the Solar Anomalous and Magnetospheric Particle Explorer (SAMPEX) at 11 UT on January 16, 2008. During the conjunction, relativistic electron microbursts were highly correlated with patchy aurora (PA), a type of pulsating aurora, that was emitted below.

2. Instrumentation

2.1. SAMPEX

The SAMPEX satellite was launched in July 1992 into a 520 – 760 km altitude, 82° inclination low Earth orbit (D. N. Baker et al., 1993; D. Baker et al., 2012). In general, SAMPEX had two pointing modes: spin and orbit rate rotation (zenith pointing) (Tsai et al., 2008). On the day of the conjunction, SAMPEX orbited at 425 – 502 km altitudes and spun at one revolution per minute, sampling both drifting and precipitating electrons.

SAMPEX's attitude was estimated at a 6-s cadence, and the pitch angle and magnetic coordinates were estimated using the International Geomagnetic Reference Field (Thébault et al., 2015, IGRF) magnetic field model.

For this study, we use the >1 MeV electron count data, taken by the Heavy Ion Large Telescope (HILT) (Klecker et al., 1993). HILT consisted of a large rectangular chamber with the aperture on one end, and 16 solid state detectors on the other. During this conjunction, the electron counts were accumulated from all of the solid state detectors at a 20 ms cadence. As described in Klecker et al. (1993), HILT had a $60\text{ cm}^2\text{sr}$ geometric factor, and a $68^\circ \times 68^\circ$ view angle, making it very sensitive to MeV electrons.

2.2. THEMIS ASI

The THEMIS all-sky imagers (ASIs) are a system of white light charged-coupled device (CCD) auroral cameras spread across Canada and Alaska (Harris et al., 2009; Mende et al., 2009). Each imager contains a fisheye lens that expands the camera's field of view to 170° , corresponding to latitudinal coverage of $\approx 9^\circ$ and longitudinal coverage of ≈ 1 h magnetic local time (MLT) (Donovan et al., 2006; Mende et al., 2009).

The 256×256 pixel images are taken at a 3-s cadence: a 1-s exposure followed by 2-s to process the image. To accurately compare the SAMPEX and THEMIS ASI time stamps, we highlight that the ASI times are recorded at the start of each exposure. To analyze the white light images, we used the THEMIS ASI sky map calibration data provided by the University of Calgary. The calibration data contain, among other things, arrays that map each pixel to an elevation and azimuth.

In this case study, we used the THEMIS ASI camera stationed in Gillam, Canada, henceforth simply referred to as Gillam. It was deployed in May 2006 to (56.354°N , 94.656°W).

2.3. Meridian Scanning Photometer

The meridian scanning photometer (MSP) at Gillam was designed to measure the latitudinal location and brightness of aurora as it passes through the meridian. The photometer contains a scanning multi-channel

filterwheel, from which we use three channels: 470.9 nm blue-line, 557.7 nm green-line, and 630 nm red-line (MPA: Meridian Photometer Array, 2005). Projected to the emission altitude, the MSP spatial resolution in magnetic latitude varies between $0.03^\circ - 0.4^\circ$. The photometer scans the meridian in 30 s. For a full description on the operation and calibration of meridian scanning photometers in general, see Unick et al. (2017).

3. Methodology

In essence, our analysis involves locating SAMPEX's footprint in each auroral image, estimating auroral intensity at this footprint, and comparing this auroral intensity with the >1 MeV electron counts observed by SAMPEX. We did this with the following four steps.

Step one: we interpolated the 6-s SAMPEX (latitude, longitude, and altitude) coordinates to the 3-s Gillam time stamps. This is important because when SAMPEX was at high elevations in the Gillam images, it rapidly traversed the field of view, thus resulting in large uncertainties in the estimated auroral intensity at the footprint.

Step two: we calculated SAMPEX footprint's location in each image. The SAMPEX position at ≈ 400 km altitude was magnetically mapped to the approximate pulsating auroral emission altitude of 90 km (we also experimented with 80–120 km mapping) using the IRBEM-Lib magnetic field library (Boscher et al., 2012) and the IGRF magnetic field model. The 90 km SAMPEX footprints, in (latitude, longitude) coordinates, were then mapped to Gillam's (azimuth, elevation) coordinates using the ASI's skymap calibration data and Python's pymap3d library (Hirsch, 2016), called by the analysis functions in aurora-asi-lib (Shumko, 2021).

Step three: we detrended the HILT count time series to reduce the effects of the SAMPEX spin. This was necessary in order to correlate only the precipitating >1 MeV microburst electrons with the aurora. We isolated the precipitating microburst electrons from other electrons that were either drifting or precipitating with a centered running median over 5 s. A similar method has been successfully used in prior studies including O'Brien et al. (2004), Blum et al. (2015), and Douma et al. (2019).

Step four: for each image, we calculated the mean auroral intensity in a 10×10 km box around the SAMPEX footprint. We then compared the auroral intensity to the detrended HILT count time series with the Pearson correlation coefficient. Since the sampling of the two instruments is different, the detrended HILT counts were averaged over the 1-s ASI exposures.

4. Results

The conjunction between SAMPEX and Gillam occurred on January 16, 2008 at 11:00 UT, during the recovery phase of a geomagnetic substorm that happened at about 10:36 UT according to the SuperMAG substorm list (Newell & Gjerloev, 2011). At this time, the Disturbance storm time (Dst) index was -17 nT, and Figure 1a shows that the Auroral Electrojet (AE) index was 568 nT. The magnitude of AE and the lower auroral electrojet index (AL) for this pulsating aurora event are consistent with those obtained by Partamies et al. (2017).

Figure 1b shows a 40-min long keogram at Gillam, and a 20-min-long Movie S1 shows the fisheye lens view of the observed pulsating aurora. Gillam observed both the amorphous pulsating aurora and PA (Grono & Donovan, 2020). Movie S1 and Figure 1b show that the PA persisted for minutes at a time while it changed shape and drifted to the East. The patchy aurora does not appear to be pulsating, but that could be due to instrumental effect that will be discussed later. Consequently, patchy aurora is classified as a type of pulsating aurora but is bewilderingly distinct from patchy pulsating aurora. Grono and Donovan (2020) argue that patchy aurora and patchy pulsating aurora are "closely related in terms of the underlying scattering mechanism responsible for the precipitation."

The SAMPEX footprint path, shown in Figure 1b by the red line, passed through the PA between $64^\circ - 66^\circ$ magnetic latitude; the PA was also observed in the MSP data shown in Figures 1c–1e. The MSP showed strong luminosity enhancements in the green and blue channels during the SAMPEX pass overhead. However, enhanced luminosity was not clearly observed in the red channel.

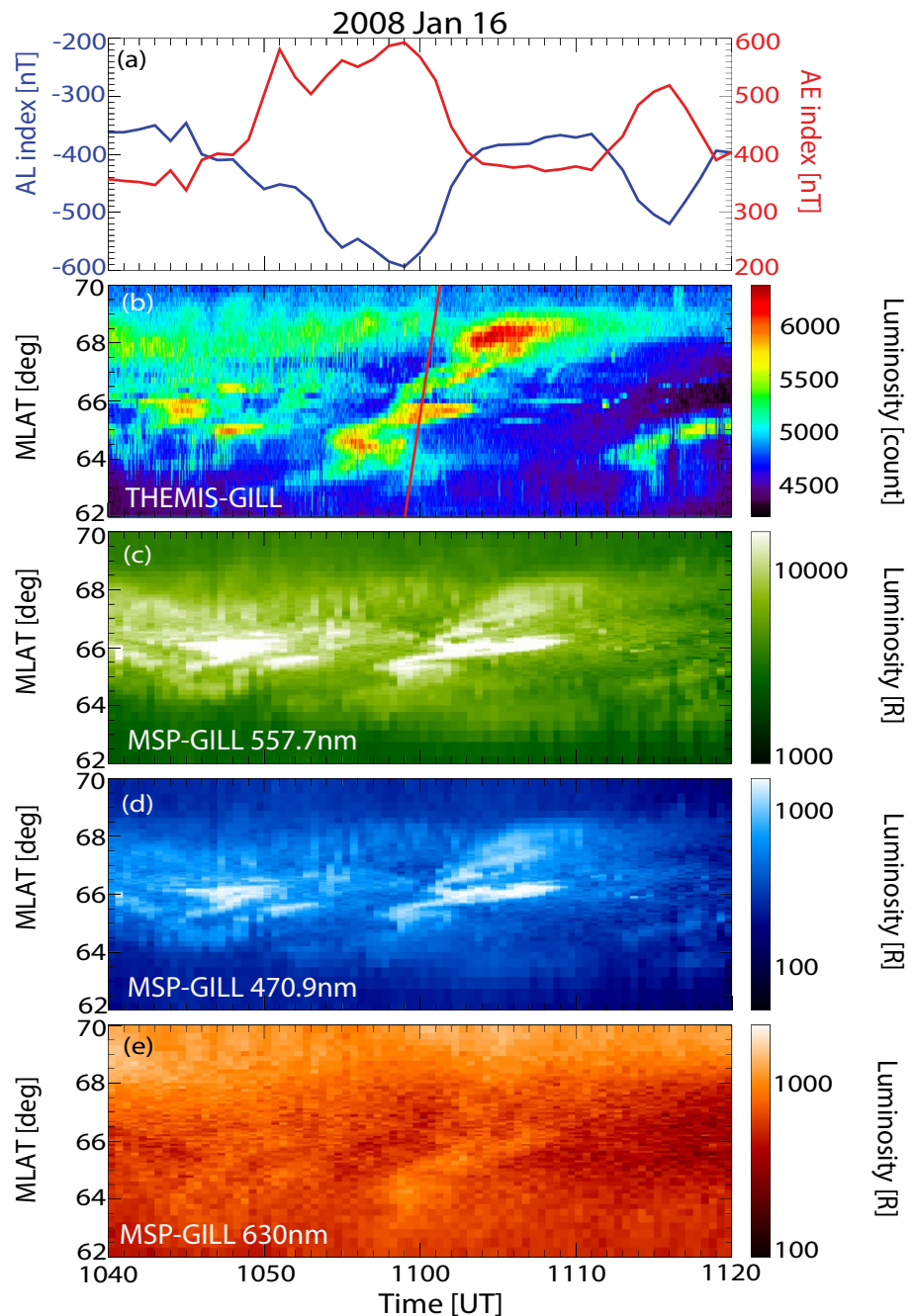


Figure 1. Ground-based observations during the conjunction on January 16, 2008. Panel (a) shows the Auroral Electrojet (AE) and AL indices (AU was close to 0 and not shown). Panel (b) shows a Gillam ASI keogram along the Solar Anomalous and Magnetospheric Particle Explorer (SAMPEX) 90 km footprint that is shown by the red line centered at 11 UT. Panels (c–e) show the meridian scanning photometer data from the 558, 471, and 630 nm channels, also taken at Gillam. Panel (b) shows that SAMPEX passed through patches of aurora as the meridian scanning photometer (MSP) observed intensified luminosity. The luminosity enhancements in the 558 and 470 nm channels, and not in the 630 nm channel, is indicative of aurora emission by 10s of keV electrons.

Now we will take a closer look around 11 UT. Movie S2 shows the SAMPEX footprint passing through two PA patches close to zenith, at 6 – 6.5 L-Shell and 4.5 h magnetic local time. Figure 2 shows a frame-by-frame 45-s montage as SAMPEX traversed Gillam’s field of view. Figures 2a–2o show the Gillam frames with the superposed SAMPEX trajectory, while Figures 2p and 2q show the time series of the auroral intensity and

2008-01-16 | SAMPEX-HILT | THEMIS-GILL

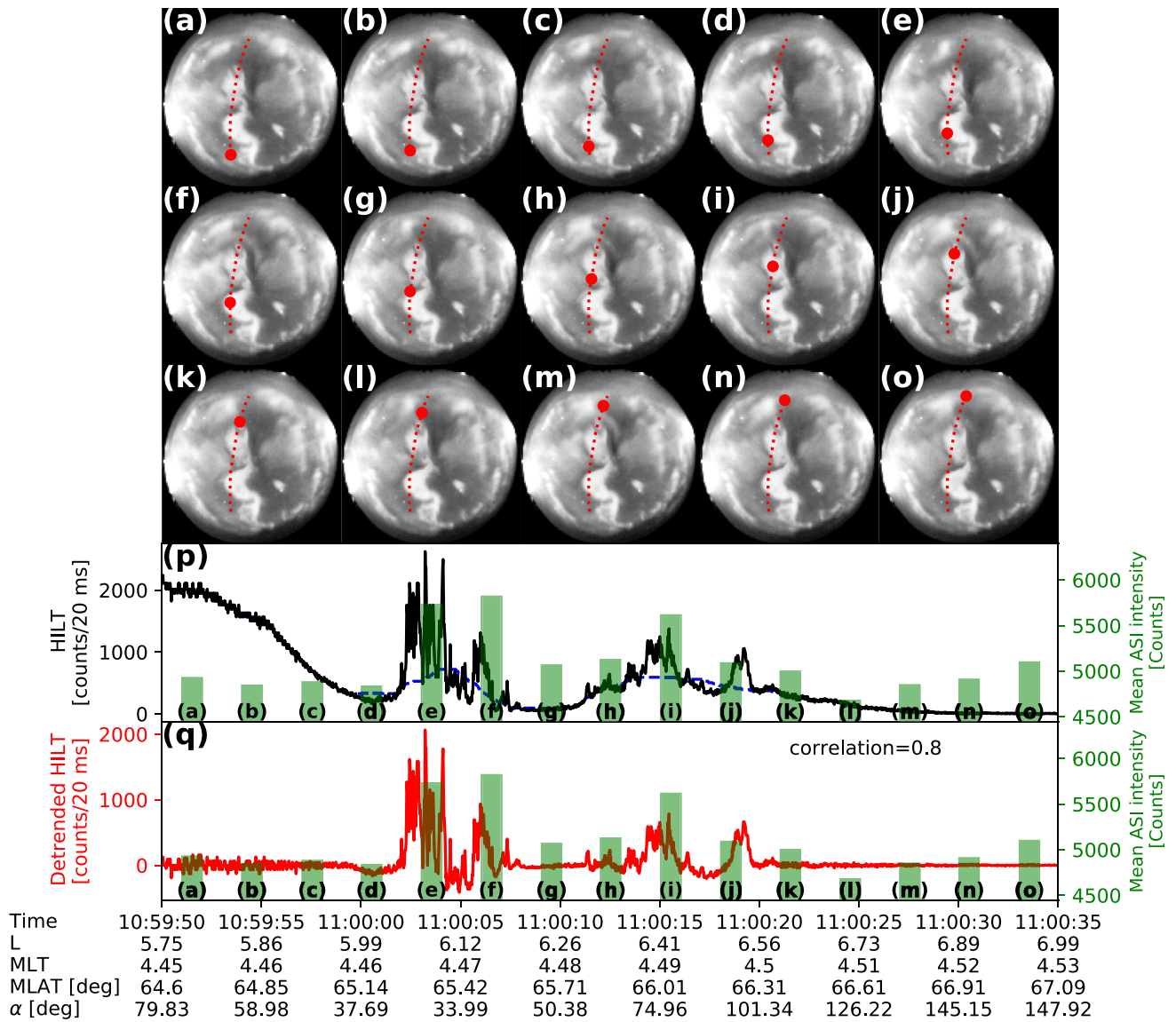


Figure 2. A 45-s conjunction montage. Panels (a–o) show the frame-by-frame dynamics of the pulsating aurora during a 45-s interval. North is toward the top and East is to the right of each frame. The 90-km altitude Solar Anomalous and Magnetospheric Particle Explorer (SAMPEX) footprint trajectory is shown by the dotted-red line, and the instantaneous SAMPEX footprint is shown by the large red circle. Panel (p) shows the original Heavy Ion Large Telescope (HILT) counts and the mean All-Sky Imager (ASI) counts at the SAMPEX footprint. The HILT count time series is shown by the black line and the running average background is shown by the dashed blue line. The green rectangles represent the mean ASI intensity with their height, and exposure duration with their width. Lastly, panel (q) is identical to panel p with the exception that it shows the detrended HILT counts. (MLT = magnetic local time, MLAT = magnetic latitude, and α = pitch angle).

HILT counts. Figure 2p shows the original HILT counts in black and Figure 2q shows the detrended HILT counts in red. In both panels, the ASI intensity time series was averaged in a 10×10 km box around the SAMPEX footprint (Figures 2a–2o) and shown by the green rectangles.

During the conjunction, SAMPEX was magnetically connected to two partially connected PA patches, part of a larger PA structure that was elongated in latitude. Concurrently, HILT measured two microburst trains. The first train at 11:00:05 consisted of about a dozen intense microbursts, while the second train at 11:00:15 consisted of a handful of relatively weak microbursts. During the first microburst train, SAMPEX was pointed at $\alpha \approx 30^\circ$ pitch angles, well inside the $\alpha = 60^\circ - 70^\circ$ loss cone. The lull at 11:00:10 in the HILT

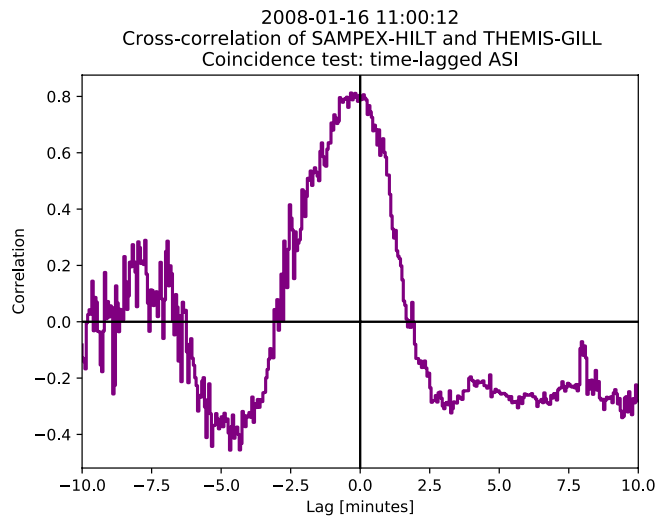


Figure 3. Heavy Ion Large Telescope (HILT)-Gillam coincidence test. The purple curve shows the cross-correlation between the detrended HILT time series and the All-Sky Imagers (ASIs) footprint intensity as a function ASI time lag. The 5-min wide peak corresponds to how long the patchy aurora convected through the Solar Anomalous and Magnetospheric Particle Explorer (SAMPEX) path.

counts corresponded to SAMPEX passing between the two PA patches. For the 45-s time interval shown in Figure 2, the correlation between the detrended HILT counts and the ASI intensity is 0.8.

To check that this correlation is a unique signature and not a coincidence, we conduct a test using the above methodology with one change: we offset (i.e., lagged) the ASI frames in time. Put simply, this test quantifies how well the microbursts observed by HILT correlate with the aurora observed at a different time, but along the same footprint path. Figure 3 shows the test result for ASI frame lags between ± 10 min. The HILT time series correlated well only for the PA that drifted through the SAMPEX footprint for ≈ 5 minutes (correlation was > 0.6 for 2 min during that time interval).

For the final check, we investigated the effect of different mapping altitudes. We repeated the above analysis with varying auroral emission altitudes spanning 80–120 km. We found that 100 km altitude maximized the correlation at 0.81, and correlation remained high from 90 – 120 km, the typical range of pulsating aurora emission altitudes (Brown et al., 1976).

5. Discussion and Conclusions

We found a significant correlation of 0.8 between precipitating > 1 MeV electron microbursts and patchy aurora. This correlation is robust to the uncertainties in the mapping altitude and timing: the correlation is sig-

nificant for the typical aurora emission altitudes of 80–120 km, and the correlation is significant for only that PA and no other aurora observed within 10 min. Thus, this correlation is unlikely due to chance.

Now we infer the lower energy bound of the precipitating electrons using the MSP data. Panels (c) and (d) in Figure 1 show that the green and blue channel luminosity, but not the red channel luminosity, was elevated near zenith at 11 UT. In principle, the three MSP channels respond uniquely to precipitating electrons: blue-line intensity is roughly proportional to the total precipitating electron energy flux and is thus more biased to the higher-energy portion of the precipitation, the green-line intensity is most responsive to electrons in the keV range, and the red-line intensity is most responsive to soft electron precipitation (< 1 keV) (Grubbs et al., 2018).

The MSP data show strong blue-line emissions for the auroral patches of interest, yet faint or even indistinguishable red-line luminosity enhancements. This suggests that the patchy aurora were emitted by energetic electron precipitation with energies > 1 keV. More quantitatively, we evaluate and show the green-to-blue line intensity ratios of the patchy auroras in Figure S1. The ratios unambiguously point to electron precipitation with mean energy > 10 keV. This is similar to the event described by Samara et al. (2015) in Section 3.1.2, where the Reimei satellite was conjugate to pulsating aurora and did not observe a corresponding enhancement of electrons in 10 eV–12 keV energies (12 keV is the instrument's upper energy limit). In our case, observations imply that the 10s keV pulsating aurora electrons were concurrent with > 1 MeV electrons, differing by two orders of magnitude in energy.

Kurita et al. (2015) presented a conjunction with a similar association of diffuse aurora with HILT counts. However, no microburst precipitation was observed during their conjunction, notably when the SAMPEX footprint passed through pulsating aurora. A more recent study by Miyoshi et al. (2021) reported an association between pulsating aurora and atmospheric ionization to altitudes as low as 65 km, likely caused by MeV electrons. The handful of studies showing correlation between the pulsating aurora and > 1 MeV electrons suggest that the conditions to scatter MeV electrons are more stringent than the conditions to scatter keV electrons, and thus are harder to find (Lee et al., 2012; Summers, 2005). Future statistical studies will investigate the association of MeV microburst electrons with diffuse aurora.

No results are without limitation and our results are no different. For this study, Gillam's 1-s exposure is one limitation worth elaborating on. Due to THEMIS ASI's 1-s exposure and 2-s processing time, we can

only confidently correlate THEMIS ASI images to a series of microbursts in quick succession (a microburst train). Correlating an individual, ≈ 100 ms duration, relativistic microburst is difficult with most camera systems. Moreover, the exposure limits us on accurately quantifying the frequency of the pulsating aurora: >1 Hz modulations are integrated over by the exposure, and <1 Hz pulsations are difficult to quantify due to the discontinuous time sampling. One possibility is that the aurora that we classified as patchy aurora could have modulated at >1 Hz frequencies with individual modulations corresponding to individual microbursts (Kataoka et al., 2012; Nishiyama et al., 2012). Nevertheless, we can confidently say that some of the aurora toggled on and off between sequential frames in Movies S1 and S2, so at least some of the aurora was aliased to a 6-s period.

We stress that the correlation between pulsating aurora and MeV electrons does not imply that the visible pulsating aurora light is emitted by MeV electrons. But this result does imply that in the pulsating aurora phenomenon, aurora-producing keV electrons are sometimes accompanied by MeV electron microbursts, both likely scattered by a similar mechanism. In energy, the simplest, yet observationally unconfirmed, energy spectrum has a continuously and exponentially decaying form for electrons spanning keV–MeV energies. This conclusion is theoretically supported by Miyoshi et al. (2020), who predicted that relativistic microbursts are the high-energy tail of the pulsating aurora.

Now, we speculate on the scattering mechanism. Our biggest assumption is that these electrons were scattered by chorus waves. Under this assumption, the long-lasting PA's light was emitted by the scattered anisotropic keV electrons that were responsible for the chorus wave instability in the chorus active region (Hikishima et al., 2010; Omura & Nunn, 2011). Under the right conditions, these chorus waves are able to interact via the cyclotron resonance with MeV electrons at $\approx 30^\circ$ magnetic latitudes, or alternatively resonating via a higher harmonic near the magnetic equator (Lorentzen, Blake, et al., 2001; Miyoshi et al., 2015; Saito et al., 2012). These waves, together with sufficient radiation belt electron flux, result in the generation of MeV microbursts.

In conclusion, we found a high correlation of 0.8 between patchy aurora and >1 MeV electron microbursts. The simplest conjecture is that the scattering mechanism responsible for pulsating aurora scatters both keV and MeV electrons, a two orders of magnitude energy difference. The precipitating keV electrons generate the visible pulsating aurora, while the associated MeV electrons penetrate deeper into the atmosphere and produce X-rays that are unobservable from the ground. This correlation, if later proved to be causation, has important implications for magnetosphere-ionosphere coupling. Furthermore, auroral observations would allow for a spatially comprehensive understanding of the effects that rapid loss of relativistic radiation belt electrons has on the atmosphere. Future work will expand this case study to multiple events, to determine under what conditions is pulsating aurora accompanied by relativistic microbursts.

Data Availability Statement

The SAMPEX HILT and attitude data are available from <http://www.srl.caltech.edu/sampex/DataCenter/data.html> and the THEMIS ASI and MSP data are available from <https://data.phys.ucalgary.ca/>. The aurora-asi-lib library is available at <https://doi.org/10.5281/zenodo.4746446>.

Acknowledgments

The authors are thankful for the engineers and scientists who made the SAMPEX and THEMIS missions possible. M. Shumko and B. Gallardo-Lacourt acknowledge the support provided by the NASA Postdoctoral Program at the NASA's Goddard Space Flight Center, administered by Universities Space Research Association under contract with NASA; and L. Blum acknowledges the Heliophysics Innovation Fund program at NASA's Goddard Space Flight Center. The authors appreciate the fruitful conversations with D. M. Klumpar.

References

- Anderson, K. A., & Milton, D. W. (1964). Balloon observations of X rays in the auroral zone: 3. High time resolution studies. *Journal of Geophysical Research*, 69(21), 4457–4479. <https://doi.org/10.1029/JZ069i021p04457>
- Baker, D., Mazur, J., & Mason, G. (2012). SAMPEX to reenter atmosphere: Twenty-year mission will end. *Space Weather*, 10(5). <https://doi.org/10.1029/2012sw000804>
- Baker, D. N., Mason, G. M., Figueroa, O., Colon, G., Watzin, J. G., & Aleman, R. M. (1993). An overview of the solar anomalous, and magnetospheric particle explorer (SAMPEX) mission. *IEEE Transactions on Geoscience and Remote Sensing*, 31(3), 531–541. <https://doi.org/10.1109/36.225519>
- Blake, J. B., Looper, M. D., Baker, D. N., Nakamura, R., Klecker, B., & Hovestadt, D. (1996). New high temporal and spatial resolution measurements by SAMPEX of the precipitation of relativistic electrons. *Advances in Space Research*, 18(8), 171–186. [https://doi.org/10.1016/0273-1177\(95\)00969-8](https://doi.org/10.1016/0273-1177(95)00969-8)
- Blum, L., Li, X., & Denton, M. (2015). Rapid MeV electron precipitation as observed by SAMPEX/HILT during high-speed stream-driven storms. *Journal of Geophysical Research: Space Physics*, 120(5), 3783–3794. <https://doi.org/10.1002/2014JA020633>
- Boscher, D., Bourdarie, S., O'Brien, P., Guild, T., & Shumko, M. (2012). *Irbem-lib library*.

- Breneman, A., Crew, A., Sample, J., Klumpar, D., Johnson, A., Agapitov, O., et al. (2017). Observations directly linking relativistic electron microbursts to whistler mode chorus: Van allen probes and FIREBIRD II. *Geophysical Research Letters*, *44*, 11265–11272. <https://doi.org/10.1002/2017gl075001>
- Brown, N., Davis, T., Hallinan, T., & Stenbaek-Nielsen, H. (1976). Altitude of pulsating aurora determined by a new instrumental technique. *Geophysical Research Letters*, *3*(7), 403–404. <https://doi.org/10.1029/gl003i007p00403>
- Chen, L., Breneman, A. W., Xia, Z., & Zhang, X.-j. (2020). Modeling of bouncing electron microbursts induced by ducted chorus waves. *Geophysical Research Letters*, *47*(17), e2020GL089400. <https://doi.org/10.1029/2020GL089400>
- Crew, A. B., Spence, H. E., Blake, J. B., Klumpar, D. M., Larsen, B. A., O'Brien, T. P., et al. (2016). First multipoint in situ observations of electron microbursts: Initial results from the NSF FIREBIRD II mission. *Journal of Geophysical Research: Space Physics*, *121*(6), 5272–5283. <https://doi.org/10.1002/2016JA022485>
- Datta, S., Skoug, R., McCarthy, M., & Parks, G. (1997). Modeling of microburst electron precipitation using pitch angle diffusion theory. *Journal of Geophysical Research*, *102*(A8), 17325–17333. <https://doi.org/10.1029/97ja00942>
- Donovan, E., Mende, S., Jackel, B., Frey, H., Syrjäsuo, M., Voronkov, I., et al. (2006). The themis all-sky imaging array: System design and initial results from the prototype imager. *Journal of Atmospheric and Solar-Terrestrial Physics*, *68*(13), 1472–1487. <https://doi.org/10.1016/j.jastp.2005.03.027>
- Douma, E., Rodger, C., Blum, L., O'Brien, T., Clilverd, M., & Blake, J. (2019). Characteristics of relativistic microburst intensity from SAMPEX observations. *Journal of Geophysical Research: Space Physics*, *124*, 5627–5640. <https://doi.org/10.1029/2019ja026757>
- Douma, E., Rodger, C. J., Blum, L. W., & Clilverd, M. A. (2017). Occurrence characteristics of relativistic electron microbursts from SAMPEX observations. *Journal of Geophysical Research: Space Physics*, *122*(8), 8096–8107. <https://doi.org/10.1002/2017JA024067>
- Duderstadt, K. A., Huang, C.-L., Spence, H. E., Smith, S., Blake, J. B., Crew, A. B., et al. (2021). Estimating the impacts of radiation belt electrons on atmospheric chemistry using firebird ii and van Allen probes observations. *Journal of Geophysical Research: Atmospheres*, *126*, e2020JD033098. <https://doi.org/10.1029/2020JD033098>
- Fang, X., Randall, C. E., Lummerzheim, D., Wang, W., Lu, G., Solomon, S. C., & Frahm, R. A. (2010). Parameterization of monoenergetic electron impact ionization. *Geophysical Research Letters*, *37*(22). <https://doi.org/10.1029/2010gl045406>
- Fukizawa, M., Sakanoi, T., Miyoshi, Y., Hosokawa, K., Shiokawa, K., Katoh, Y., et al. (2018). Electrostatic electron cyclotron harmonic waves as a candidate to cause pulsating auroras. *Geophysical Research Letters*, *45*(23), 12–661. <https://doi.org/10.1029/2018gl080145>
- Grono, E., & Donovan, E. (2020). Surveying pulsating auroras. *Annales geophysicae*, 1–8. <https://doi.org/10.5194/angeo-38-1-2020>
- Grubbs, G., Michell, R., Samara, M., Hampton, D., Hecht, J., Solomon, S., & Jahn, J.-M. (2018). A comparative study of spectral auroral intensity predictions from multiple electron transport models. *Journal of Geophysical Research: Space Physics*, *123*(1), 993–1005. <https://doi.org/10.1002/2017ja025026>
- Harris, S., Mende, S., Angelopoulos, V., Rachelson, W., Donovan, E., Jackel, B., et al. (2009). Themis ground based observatory system design. *The THEMIS Mission*, *141*, 213–233. https://doi.org/10.1007/978-0-387-89820-9_10
- Hikishima, M., Omura, Y., & Summers, D. (2010). Microburst precipitation of energetic electrons associated with chorus wave generation. *Geophysical Research Letters*, *37*(7). <https://doi.org/10.1029/2010gl042678>
- Hirsch, M. (2016). *Pymap3d: Python 3d coordinate conversions for geospace*. <https://doi.org/10.5281/zenodo.213676>
- Hoffman, R. A., & Evans, D. S. (1968). Field-aligned electron bursts at high latitudes observed by OGO 4. *Journal of Geophysical Research*, *73*(19), 6201–6214. <https://doi.org/10.1029/ja073i019p06201>
- Hofmann, D., & Greene, R. (1972). Balloon observations of simultaneous auroral x-ray and visible bursts. *Journal of Geophysical Research*, *77*(4), 776–780. <https://doi.org/10.1029/ja077i004p00776>
- Horne, R. B., Thorne, R. M., Glauert, S. A., Albert, J. M., Meredith, N. P., & Anderson, R. R. (2005). Timescale for radiation belt electron acceleration by whistler mode chorus waves. *Journal of Geophysical Research*, *110*(A3). <https://doi.org/10.1029/2004ja010811>
- Jaynes, A., Lessard, M., Rodriguez, J., Donovan, E., Loto'Aniu, T., & Rychert, K. (2013). Pulsating auroral electron flux modulations in the equatorial magnetosphere. *Journal of Geophysical Research*, *118*(8), 4884–4894. <https://doi.org/10.1002/jgra.50434>
- Johnstone, A. (1978). Pulsating aurora. *Nature*, *274*(5667), 119–126. <https://doi.org/10.1038/274119a0>
- Jones, S., Lessard, M., Rychert, K., Spanswick, E., Donovan, E., & Jaynes, A. (2013). Persistent, widespread pulsating aurora: A case study. *Journal of Geophysical Research*, *118*(6), 2998–3006. <https://doi.org/10.1002/jgra.50301>
- Kasahara, S., Miyoshi, Y., Yokota, S., Mitani, T., Kasahara, Y., Matsuda, S., et al. (2018). Pulsating aurora from electron scattering by chorus waves. *Nature*, *554*(7692), 337. <https://doi.org/10.1038/nature25505>
- Kataoka, R., Miyoshi, Y., Hampton, D., Ishii, T., & Kozako, H. (2012). Pulsating aurora beyond the ultra-low-frequency range. *Journal of Geophysical Research*, *117*(A8). <https://doi.org/10.1029/2012ja017987>
- Klecker, B., Hovestadt, D., Scholer, M., Arbing, H., Ertl, M., Kastele, H., et al. (1993). HILT: A heavy ion large area proportional counter telescope for solar and anomalous cosmic rays. *IEEE Transactions on Geoscience and Remote Sensing*, *31*(3), 542–548. <https://doi.org/10.1109/36.225520>
- Kurita, S., Kadokura, A., Miyoshi, Y., Morioka, A., Sato, Y., & Misawa, H. (2015). Relativistic electron precipitations in association with diffuse aurora: Conjugate observation of SAMPEX and the all-sky Tv camera at Syowa station. *Geophysical Research Letters*, *42*(12), 4702–4708. <https://doi.org/10.1002/2015gl064564>
- Lee, J. J., Parks, G. K., Lee, E., Tsurutani, B. T., Hwang, J., Cho, K. S., et al. (2012). Anisotropic pitch angle distribution of 100 keV microburst electrons in the loss cone: Measurements from STSAT-1. *Annales Geophysicae*, *30*(11), 1567–1573. <https://doi.org/10.5194/angeo-30-1567-2012>
- Lessard, M. (2012). A review of pulsating aurora. *Auroral phenomenology and magnetospheric processes: Earth and other planets* (pp. 55–68).
- Li, J., Bortnik, J., An, X., Li, W., Angelopoulos, V., Thorne, R. M., et al. (2019). Origin of two-band chorus in the radiation belt of earth. *Nature Communications*, *10*(1), 1–9. <https://doi.org/10.1038/s41467-019-12561-3>
- Lorentzen, K. R., Blake, J. B., Inan, U. S., & Bortnik, J. (2001). Observations of relativistic electron microbursts in association with VLF chorus. *Journal of Geophysical Research*, *106*(A4), 6017–6027. <https://doi.org/10.1029/2000JA003018>
- Lorentzen, K. R., Looper, M. D., & Blake, J. B. (2001). Relativistic electron microbursts during the GEM storms. *Geophysical Research Letters*, *28*(13), 2573–2576. <https://doi.org/10.1029/2001GL012926>
- Mende, S., Harris, S., Frey, H., Angelopoulos, V., Russell, C., Donovan, E., et al. (2009). The THEMIS array of ground-based observatories for the study of auroral substorms. *The THEMIS Mission*, *141*, 357–387. https://doi.org/10.1007/978-0-387-89820-9_16
- Meridian Photometer Array. (2005). Retrieved from <https://aurora.phys.ucalgary.ca/norstar/msp/inst.html>
- Millan, R., & Thorne, R. (2007). Review of radiation belt relativistic electron losses. *Journal of Atmospheric and Solar-Terrestrial Physics*, *69*(3), 362–377. <https://doi.org/10.1016/j.jastp.2006.06.019>

- Miyoshi, Y., Hosokawa, K., Kurita, S., Oyama, S.-I., Ogawa, Y., Saito, S., et al. (2021). Penetration of MeV electrons into the mesosphere accompanying pulsating aurorae. *Scientific Reports*, *11*(1), 1–9. <https://doi.org/10.1038/s41598-021-92611-3>
- Miyoshi, Y., Oyama, S., Saito, S., Kurita, S., Fujiwara, H., Kataoka, R., et al. (2015). Energetic electron precipitation associated with pulsating aurora: Eiscat and Van allen probe observations. *Journal of Geophysical Research: Space Physics*, *120*(4), 2754–2766. <https://doi.org/10.1002/2014ja020690>
- Miyoshi, Y., Saito, S., Kurita, S., Asamura, K., Hosokawa, K., Sakanoi, T., et al. (2020). Relativistic electron microbursts as high energy tail of pulsating aurora electrons. *Geophysical Research Letters*, *41*. <https://doi.org/10.1029/2020GL090360>
- Newell, P., & Gjerloev, J. (2011). Evaluation of supermag auroral electrojet indices as indicators of substorms and auroral power. *Journal of Geophysical Research*, *116*(A12). <https://doi.org/10.1029/2011ja016779>
- Nishimura, Y., Bortnik, J., Li, W., Thorne, R. M., Lyons, L. R., Angelopoulos, V., et al. (2010). Identifying the driver of pulsating aurora. *Science*, *330*, 81–84. <https://doi.org/10.1126/science.1193186>
- Nishiyama, T., Sakanoi, T., Miyoshi, Y., Kataoka, R., Hampton, D., Katoh, Y., et al. (2012). Fine scale structures of pulsating auroras in the early recovery phase of substorm using ground-based EMCCD camera. *Journal of Geophysical Research*, *117*(A10). <https://doi.org/10.1029/2012ja017921>
- O'Brien, T. P., Looper, M. D., & Blake, J. B. (2004). Quantification of relativistic electron microburst losses during the GEM storms. *Geophysical Research Letters*, *31*(4), L04802. <https://doi.org/10.1029/2003GL018621>
- O'Brien, T. P., Lorentzen, K. R., Mann, I. R., Meredith, N. P., Blake, J. B., Fennell, J. F., & Anderson, R. R. (2003). Energization of relativistic electrons in the presence of ULF power and MeV microbursts: Evidence for dual ULF and VLF acceleration. *Journal of Geophysical Research*, *108*(A8). <https://doi.org/10.1029/2002JA009784>
- Oliven, M. N., & Gurnett, D. A. (1968). Microburst phenomena: 3. An association between microbursts and VLF chorus. *Journal of Geophysical Research*, *73*(7), 2355–2362. <https://doi.org/10.1029/JA073i007p02355>
- Omura, Y., & Nunn, D. (2011). Triggering process of whistler mode chorus emissions in the magnetosphere. *Journal of Geophysical Research*, *116*(A5). <https://doi.org/10.1029/2010ja016280>
- Partamies, N., Whiter, D., Kadokura, A., Kauristie, K., Nesse Tysøy, H., Massetti, S., & Raita, T. (2017). Occurrence and average behavior of pulsating aurora. *Journal of Geophysical Research: Space Physics*, *122*(5), 5606–5618. <https://doi.org/10.1002/2017ja024039>
- Ripoll, J.-F., Claudepierre, S., Ukhorskiy, A., Colpitts, C., Li, X., Fennell, J., & Crabtree, C. (2020). Particle dynamics in the earth's radiation belts: Review of current research and open questions. *Journal of Geophysical Research: Space Physics*, *125*(5), e2019JA026735. <https://doi.org/10.1029/2019ja026735>
- Royrvik, O., & Davis, T. (1977). Pulsating aurora: Local and global morphology. *Journal of Geophysical Research*, *82*(29), 4720–4740. <https://doi.org/10.1029/ja082i029p04720>
- Saito, S., Miyoshi, Y., & Seki, K. (2012). Relativistic electron microbursts associated with whistler chorus rising tone elements: GEM-SIS-RBW simulations. *Journal of Geophysical Research*, *117*(A10), A10206. <https://doi.org/10.1029/2012JA018020>
- Samara, M., Michell, R., & Redmon, R. (2015). Low-altitude satellite measurements of pulsating auroral electrons. *Journal of Geophysical Research: Space Physics*, *120*(9), 8111–8124. <https://doi.org/10.1002/2015ja021292>
- Sandahl, I., Eliasson, L., & Lundin, R. (1980). Rocket observations of precipitating electrons over a pulsating aurora. *Geophysical Research Letters*, *7*(5), 309–312. <https://doi.org/10.1029/gl007i005p00309>
- Shumko, M. (2021). *Aurora-asi-lib: Easily download, plot, animate, and analyze aurora all sky imager (ASI) data*. <https://doi.org/10.5281/zenodo.4746446>
- Shumko, M., Johnson, A., Sample, J., Griffith, B. A., Turner, D. L., O'Brien, T. P., et al. (2020). Electron microburst size distribution derived with AeroCube-6. *Journal of Geophysical Research: Space Physics*, *125*, e2019JA027651. <https://doi.org/10.1029/2019ja027651>
- Summers, D. (2005). Quasi-linear diffusion coefficients for field-aligned electromagnetic waves with applications to the magnetosphere. *Journal of Geophysical Research*, *110*(A8), A08213. <https://doi.org/10.1029/2005JA011159>
- Tesema, F., Partamies, N., Tysøy, H. N., Kero, A., & Smith-Johnsen, C. (2020). Observations of electron precipitation during pulsating aurora and its chemical impact. *Journal of Geophysical Research: Space Physics*, *125*(6), e2019JA027713. <https://doi.org/10.1029/2019ja027713>
- Thébault, E., Finlay, C. C., Beggan, C. D., Alken, P., Aubert, J., Barrois, O., et al. (2015). International geomagnetic reference field: The 12th generation. *Earth Planets and Space*, *67*(1), 79. <https://doi.org/10.1186/s40623-015-0313-0>
- Thorne, R. M., Ni, B., Tao, X., Horne, R. B., & Meredith, N. P. (2010). Scattering by chorus waves as the dominant cause of diffuse auroral precipitation. *Nature*, *467*(7318), 943–946. <https://doi.org/10.1038/nature09467>
- Thorne, R. M., O'Brien, T. P., Shprits, Y. Y., Summers, D., & Horne, R. B. (2005). Timescale for MeV electron microburst loss during geomagnetic storms. *Journal of Geophysical Research*, *110*(A9), A09202. <https://doi.org/10.1029/2004JA010882>
- Tsai, D., Markley, F., & Watson, T. (2008). Sampex spin stabilized mode. *Spaceops 2008 conference* (p. 3435). <https://doi.org/10.2514/6.2008-3435>
- Tsurutani, B. T., & Lakhina, G. S. (1997). Some basic concepts of wave-particle interactions in collisionless plasmas. *Reviews of Geophysics*, *35*(4), 491–501. <https://doi.org/10.1029/97rg02200>
- Tsurutani, B. T., Lakhina, G. S., & Verkhoglyadova, O. P. (2013). Energetic electron (>10 keV) microburst precipitation, ~5–15 s x-ray pulsations, chorus, and wave-particle interactions: A review. *Journal of Geophysical Research*, *118*(5), 2296–2312. <https://doi.org/10.1002/jgra.50264>
- Unick, C. W., Donovan, E., Connors, M., & Jackel, B. (2017). A dedicated h-beta meridian scanning photometer for proton aurora measurement. *Journal of Geophysical Research: Space Physics*, *122*(1), 753–764. <https://doi.org/10.1002/2016ja022630>
- Woodger, L., Halford, A., Millan, R., McCarthy, M., Smith, D., Bowers, G., et al. (2015). A summary of the BARREL campaigns: Technique for studying electron precipitation. *Journal of Geophysical Research: Space Physics*, *120*(6), 4922–4935. <https://doi.org/10.1002/2014ja020874>